First-principles calculations of surface *H* centers in BaF_2

H. Shi
School of Science, Beijing Institute of Technology, 100081 Beijing, People's Republic of China

R. Jia*
Bergische Universität Wuppertal, D-42097 Wuppertal, Germany

R. I. Eglitis
Institute of Solid State Physics, University of Latvia, 8 Kengaraga Str., Riga LV1067, Latvia

(Received 17 December 2009; revised manuscript received 16 March 2010; published 3 May 2010)

H center, a hole trapped at an interstitial anion site, placed on the (111) surface of Barium fluoride BaF_2 has been studied by using density functional theory (DFT) with hybrid exchange potentials, namely, DFT-B3PW. Two different configurations of surface *H* center are investigated carefully. Both surface *H*-center systems have strong relaxations because of the surface effect. In the configuration that the interstitial fluorine atom is within the surface, named case 1 in this paper, the unpaired electron is almost equally distributed onto the two atoms of the *H* center, which is quite different from the bulk *H*-center case. The other configuration with one of the F atoms of the *H* center located above the BaF_2 (111) surface (case 0) has a more polarized charge distribution as compared to that obtained in the bulk case and case 1. The calculation on total energies of different surface *H*-center configurations implies that *H* centers have a trend to locate near the surface. The creation of a surface *H* center in BaF_2 results in a new β-hole band located at the Γ point 3.99 and 2.70 eV, for the cases 0 and 1, respectively, above the top of valence bands. According to our calculations on density of states, the constituents of the defect bands are cleared and the β-hole band is primarily composed of p_z orbitals localized on the *H* center.

DOI: 10.1103/PhysRevB.81.195101 PACS number(s): 71.15.Mb, 71.20.−b, 73.20.Hb, 68.43.Fg

I. INTRODUCTION

Alkaline-earth fluorides such as CaF_2 and BaF_2 whose band gaps are larger than 10 eV, are very important for many optical applications. As an example, a recent demand for lens materials available in short wavelength lithography is a typical application. The currently targeted wavelength is 157 nm (about 8 eV) from an F_2-excimer laser. This wavelength is far shorter than the transparent region of quartz that is the most popular optical material in the ultraviolet (UV) region. Additionally, for BaF_2 it is the fastest luminescent material that has been found to date.[1] Recently, BaF_2 has also been found to exhibit superionic conductivity by dissolving appropriate impurities into the lattice or by introducing an interface that causes the redistribution of ions in the space charge region, and is therefore considered as a candidate material for high-temperature batteries, fuel cells, chemical filters and sensors.[2] Considering the high technological importance of alkaline-earth fluorides, it is not surprising that during the last years, they have been the subject of many experimental and theoretical studies.[3–24] It is well-known that optical and mechanical properties of crystals are strongly affected by defects and impurities unavoidably present in any real material. Contemporary knowledge of defects in solids has helped to create a field of technology, namely, *defect engineering*, which is aimed at manipulating the nature and concentration of defects in a material so as to tune its properties in a desired manner or to generate different behaviors. BaF_2 could become important optical materials if one could avoid or, at least, control the photoinduced defect formation, which so far in applications degrades its optical quality. Therefore, it is significative to understand the nature of defects in BaF_2.

A kind of important point defect, *H* center (a hole trapped at an interstitial anion site), which is relevant and similar to the V_k center, a self-trapped hole, is readily formed in crystals doped with the heavier trivalent rare-earth ions (such as Re^{3+}). *H* centers produced by *X*-irradiation of rare-earth doped crystals have been identified in CaF_2 by Hall *et al.*[25] and in CaF_2, SrF_2, and BaF_2 by Beaumont *et al.*[26] In suitably grown crystals these ions introduce charge-compensating fluorine interstitials (F_i^-) and a fraction of these are not closely associated with the rare-earth ions. When such crystals are *X*-irradiated at 77 K large concentrations of V_k centers are produced and a relatively small concentration of *H* centers. However, when the crystals are heated to induce migration of V_k centers a fraction of the moving holes are retrapped at F_i^- sites producing additional *H* centers. The hole is located on the interstitial fluorine and a nearest substitutional fluorine giving a (111) oriented molecular ion (X_2^-). *H* centers may also be produced in undoped alkaline-earth fluorides by heavy irradiation with 1 MeV electrons at 77 K. In some orientations of the external magnetic field the electron paramagnetic resonance lines of *H* centers produced by electron irradiation show partly resolved structure suggesting perturbation by another defect produced by the radiation.[27] For the optical absorption, Beaumont *et al.* found evidence for the existence of an absorption band of the *H* center peaking at about 4.03 eV in CaF_2 and 3.76 eV in BaF_2.[26]

As an extension of our previous study dealing with *H* centers in alkaline-earth fluoride bulks,[28] we performed calculations for BaF_2 surface *H* centers. The atomic and electronic structure of surface *H* centers, is practically unknown, and according to our knowledge has never been addressed in

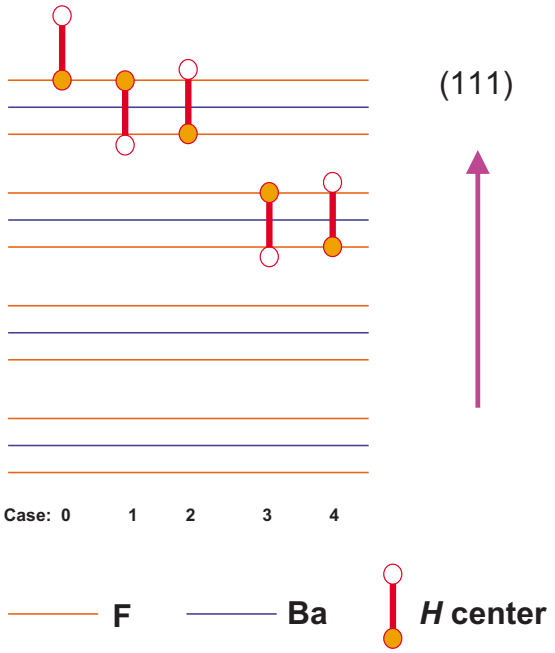

FIG. 1. (Color online) Schematic sketch of the (111) slab containing *H* centers. The solid and hollow circles denote substitutional (H1) and interstitial (H2) fluorine atoms, respectively.

literature. In the present work, we have studied surface *H* centers on the (111) surface, which is the most stable one among the (111), (110), and (100) terminated surfaces according to our previous researches[20,21] about the pure alkaline-earth fluoride slabs. The structure of the alkaline-earth fluoride (111) surface is illustrated in Fig. 1. Each layer has three sublayers forming a fluorine-metal-fluorine (F-M-F) layer structure. We performed our surface *H*-center investigations for a slab containing four layers. Each layer consists of three sublayers, containing nine atoms. Thereby we preformed the surface *H*-center calculations for supercells containing 108 atoms. Actually, there are 109 atoms in the system being due to the *H* center including two atoms. In the present study, *ab initio* calculations were made for 5 different BaF_2 surface *H*-center configurations. The geometrical relaxations, stable properties and electronic structures of surface *H* centers are presented. The effect of the surface on specific quantities such as *H*-center lengths, effective charges, or on the band structure with respect to that calculated for the bulk case[28] are also shown and discussed.

II. CALCULATION METHODS

To investigate surface *H* centers in BaF_2 we used the first-principles density functional theory (DFT)-B3PW method, according to our previous study dealing with CaF_2, BaF_2, and SrF_2 perfect crystals, which gave the best agreement with experiments for the lattice constant, bulk modulus, and optical band gap. All numerical calculations of surface *H* centers in BaF_2 were performed by the CRYSTAL-2006 computer code.[29] The CRYSTAL-2006 code employs Gaussian-type functions (GTF) localized at atoms as the basis for an expansion of the crystalline orbitals. In order to employ the linear

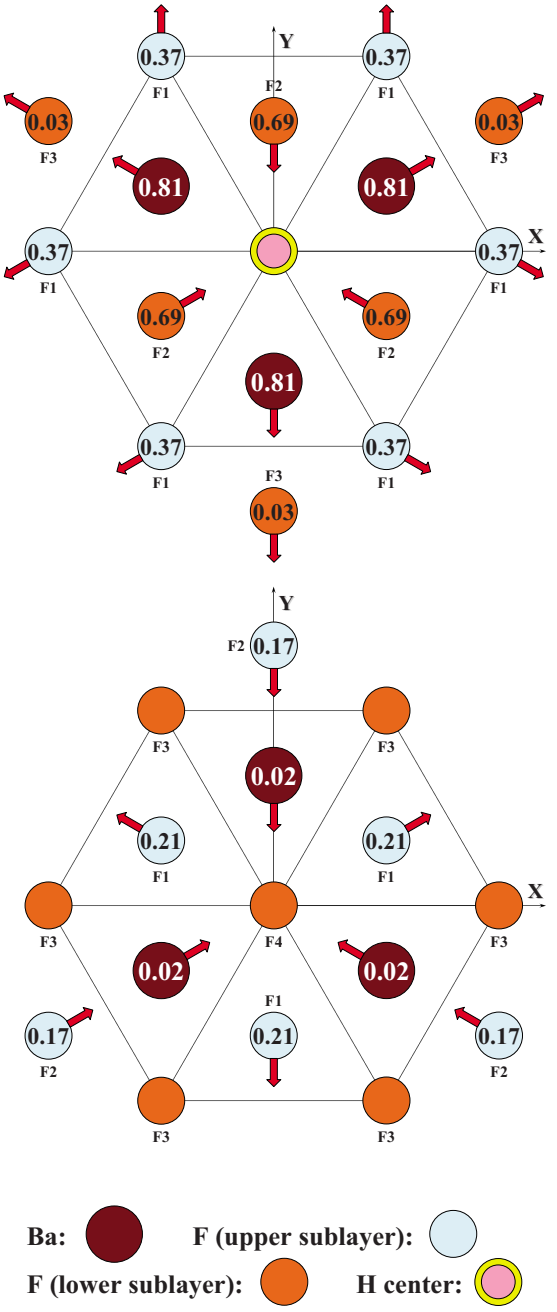

FIG. 2. (Color online) A top view of the surface *H*-center nearest-neighbor geometry with a indication of relaxation shifts for the case 0. The directions of atomic displacements in the *XY* plane are shown with arrows, the values are given as percentage of the lattice constant a_0 in circles. The fluorine atoms in different shells are labeled F1, F2, F3, and F4. The upper and lower panels denote the first layer and second layer of the (111) BaF_2 slab, respectively.

combination of atomic orbitals (LCAO)-GFT method, it is desirable to have optimized basis sets (BS). In our calculations for fluorine atoms, we applied the basis set developed by Catti *et al.*[5] For Ba, the BS optimization for $BaTiO_3$ perovskite was developed and discussed in Piskunov *et al.*[30] and Eglitis *et al.*[31] The Hay-Wadt small-core effective core pseudopotential (ECP) was adopted for the Ba atom.[32] The small-core ECP replaces only inner core orbitals, but orbitals

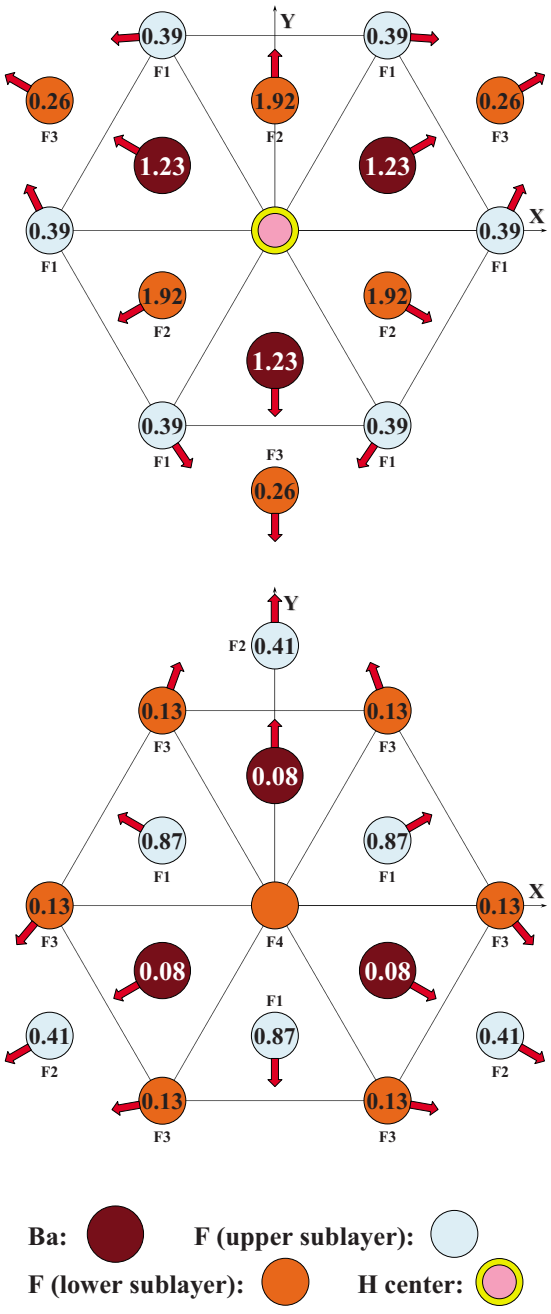

FIG. 3. (Color online) A top view of the surface *H*-center nearest-neighbor geometry with a indication of relaxation shifts for the case 1. The directions of atomic displacements in the *XY* plane are shown with arrows, the values are given as percentage of the lattice constant a_0 in circles. The fluorine atoms in different shells are labeled F1, F2, F3, and F4. The upper and lower panels denote the first layer and second layer of the (111) BaF_2 slab, respectively.

for subvalence electrons as well as for valence electrons are calculated self-consistently. In this paper, we used this BS for Ba. The basis sets are believed to be transferable, so that, once determined for some chemical constituents, they may be applied successfully in calculations for a variety of chemical substances where the latter participates.

The reciprocal space integration was performed by sampling the two-dimensional (2D) Brillouin zone of the 108-atom supercell with 6×6 Pack-Monkhorst net.[33] The thresholds N (i.e., the calculation of integrals with an accuracy of 10^{-N}) in our calculations were chosen as a compromise between the accuracy of calculations and the large computational time for large supercells. They are 7, 7, 7, 7, and 14 for the Coulomb overlap, Coulomb penetration, exchange overlap, the first-exchange pseudo-overlap, and the second-exchange pseudo-overlap, respectively.[34] BaF_2 is high ionic large-gap insulator with an $Fm\bar{3}m$ structure. The Ba^{2+} locates at the origin point in a three-atom face-centered-cubic (fcc) unit cell and two F^- at the diagonal points $(\pm\frac{1}{4},\pm\frac{1}{4},\pm\frac{1}{4})a_0$, where a_0 is the lattice constant. In our calculations, we use the theoretical optimized value of 6.26 Å from our former work.[21]

To simulate a surface *H*-center system, we created a 108-atom (111) slab including four F-Ba-F layers. Each layer unit cell is magnified up to a 3×3 2D supercell containing 27 atoms. After the interstitial fluorine atom is added, becoming a 109-atom supercell, the atomic configuration of surrounding atoms is reoptimized via a search for the total energy minimum as a function of the atomic displacements from the regular lattice sites. In our calculations, we set the free relaxation for the upper three layers (including 82 atoms) and fix the bottom layer. The *H* center with F_2^- style has the same charge as the substituted F^- in the ideal ionic case, so the supercell is neutral in our calculations and the electrostatic potential interactions between the neighboring defect supercells are eliminable. Finally, we should stress here that the two atoms in an *H* center are labeled H1 and H2 in this paper. H1 denotes the substitutional fluorine atom and H2 the interstitial fluorine atom.

III. RESULTS AND DISCUSSION

A. Geometrical properties

For a (111) slab of BaF_2 there are three sublayers in each layer from the side view, so an *H* center located on one F-Ba-F layer has two configurations. We calculated four cases of surface *H* center, corresponding to the H1 atom locating at No. 1, 3, 4, and 6 sublayer, respectively, as we can see in Fig. 1. Additionally, we also investigated F-atom adsorption on the (111) surface. A fluorine atom locates above a surface F atom, forming a surface *H* center named case 0, which is different from other cases. First, we evaluated the adsorption energy computed by subtracting the energies of the optimized 108-atom (111) perfect slab and an isolated fluorine atom from the energy of the optimized 109-atom (111) slab containing an *H* center, i.e., the case 0, as shown in the following formula:

$$E_{\mathrm{ad}} = E_H^{(n+1)} - E_F^{(1)} - E_{\mathrm{perfect}}^{(n)}, \tag{1}$$

where $E_F^{(1)}$ denotes the total energy of an isolated fluorine atom, and $E_H^{(n+1)}$ and $E_{\mathrm{perfect}}^{(n)}$ the total energies of the slab with and without an *H* center, respectively. Our calculated adsorption energy is −0.55 eV, and with the definition of Eq. (1), the negative E_{ad} corresponds to stable adsorption. For BaF_2 we found that the energetically most favorable case for surface *H* center is the case 0. The total energies of the cases 1,

TABLE I. Atomic relaxations of BaF_2 slabs containing H centers located at the (111) surface (as a percentage of the lattice constant: 6.26 Å) for the cases 0 and 1. Positive signs correspond to outward atomic displacements (toward the vacuum). The directions of atomic displacements in the XY plane are indicated in Figs. 2 and 3. The relaxations of surface H centers for the cases 0, 1, 2, 3, and 4 are also shown here.

			Case 0		Case 1	
Layer	Atoms	Number	XY (% a_0)	Z (% a_0)	XY (% a_0)	Z (% a_0)
No.1	F1	6	0.37	−0.78	0.39	−0.35
	Ba	3	0.81	+0.65	1.23	−0.61
	F2	3	0.69	+0.16	1.92	+0.28
	F3	3	0.03	−0.12	0.26	−0.49
No.2	F1	3	0.21	+0.93	0.87	+0.31
	F2	3	0.17	+0.91	0.41	+1.17
	Ba	3	0.02	+0.40	0.08	+0.64
	F3	6	<0.01	+0.04	0.13	+0.04
	F4	1	0.00	−0.06	0.00	+0.08

	Atoms	Case 0	Case 1	Case 2	Case 3	Case 4
	H1 (Z % a_0)	−1.63	+3.62	+1.62	+0.31	+0.30
H center	H Length (A)	1.98	1.97	2.01	1.99	1.99

2, 3, and 4 are larger than that of the case 0 by 0.07, 0.28, 0.39, and 0.35 eV, respectively. It implicates a trend of H centers locating near the surface. However, the energy differences of these cases are all smaller than the absolute value of E_{ad}, suggesting that the interstitial fluorine atom is not inclined to move away from the surface in despite of the trend of H centers to the surface. The cases 0 and 1 have closed total energies and are more stable than other deeper-layer H-center systems, therefore, we mainly focus our current paper on the investigation of the cases 0 and 1.

The relaxations of atoms nearest to the surface H centers are calculated and depicted in Figs. 2 and 3 and Table I. According to our previous work regarding the bulk H-center system,[28] the lengths of H center, i.e., distance between H1 and H2, in CaF_2 and BaF_2 are both 1.98 Å. The BaF_2 surface H-center lengths for the cases 0, 1, 2, 3, and 4 are 1.98, 1.97, 2.01, 1.99, and 1.99 Å, respectively, being very close to the value in the bulk H-center system. We can conclude that there is little surface effect on the length of surface H center. The Ba atoms located at the middle sublayer of the first surface layer are repulsed from the H center (H1) by 0.08% and 2.71% of a_0 for the cases 0 and 1, respectively, indicating larger distances between H1 and Ba after relaxations. We found that barium shifts along the Z axis in these two cases have opposite directions and the H center in the case 0 has a upward pulling force on the barium atoms. Due to this pulling force, the repulsion of the case 0 is much weaker than that of the case 1. On the other hand, the Ba displacements (1.04% and 1.37% of a_0 for the cases 0 and 1, respectively) are bigger than that in the bulk H-center system (0.99% of a_0).[28] The F atoms in the lower sublayer of the first surface layer (labeled No.1-F2 in Fig. 3 and Table I) for the case 1 have a larger shift of 1.94% of a_0 backward the H center than that of the bulk H-center case (1.20% of a_0)[28] by about 60% due to the surface effect. However, for the case 0, these three F atoms move toward the H center (see Fig. 2). The analysis of the position of the surface H center shows that the surface H center has a remarkable outward relaxation toward the vacuum. For the case 1, the H1 atom shifts outwards by 3.62% of a_0 with respect to its position of the unrelaxed slab whereas other F atoms in the surface top sublayer move inwards like the perfect alkaline-earth fluoride (111) surface case due to the surface effect, and the H2 atom even locates above the lower fluorine sublayer of the top layer. Other cases 2, 3, and 4 also show that the H1 atom has a upward shift and implicate that H centers in BaF_2 trend to move outwards. Unlike all of other cases, the H1 atom of the case 0 moves inward by 1.63% of a_0. Considering almost the whole H center is outside of the surface, this reversed penetration is reasonable.

B. Electronic properties

Table II presents the effective charges and spins of the surface H center and surrounding atoms for the BaF_2 (111) surface cases 0 and 1. According to our previous work about H centers in bulk,[28] the H1 and H2 charges in BaF_2 are $-0.621e$ and $-0.339e$, respectively. The total charge of the H center is not distributed equally between two F atoms and the hole is mainly located on the interstitial fluorine. However, for the surface H-center case 1, the effective charges of H1 and H2 are so closed that we cannot indicate definitely on which fluorine atom the hole is located. Because of the surface effect, the total charge of the surface H center ($-0.947e$) is smaller than that of the bulk H center ($-0.960e$)[28] by $0.013e$ and the electrons belonging to the

TABLE II. The effective charges $[Q(e)]$ of BaF_2 slabs containing *H* centers located at the (111) surface for the cases 0 and 1. ΔQ labels the change in the effective charge compared to perfect BaF_2 crystal ($Q_{Ba}=+1.845e$, $Q_F=-0.923e$ in BaF_2).[21] Spin is the result of the spin difference of electrons with different spin directions $(n_\alpha - n_\beta)$ also in unit (e). The symbols in Atoms columns are defined by Figs. 2 and 3. The effective charges and spins of surface *H* centers in the cases 0, 1, 2, 3, and 4 are also shown here.

			Case 0			Case 1		
Layer	Atoms	Number	Q (e)	$\Delta Q(e)$	Spin	Q (e)	$\Delta Q(e)$	Spin
No.1	F1	6	−0.915	+0.008	0	−0.918	+0.005	0
	Ba	3	+1.839	−0.006	0	+1.835	−0.010	−0.002
	F2	3	−0.921	+0.002	0	−0.915	+0.008	0
	F3	3	−0.921	+0.002	0	−0.920	+0.003	0
No.2	F1	3	−0.921	+0.002	0	−0.916	+0.007	+0.001
	F2	3	−0.922	+0.001	0	−0.921	+0.002	0
	Ba	3	+1.848	+0.003	0	+1.850	+0.005	0
	F3	6	−0.924	−0.001	0	−0.924	−0.001	0
	F4	1	−0.925	−0.002	0	−0.923	0.000	0
	Atoms	Charges (e)	Case 0	Case 1	Case 2	Case 3	Case 4	
H center	H1	Q	−0.698	−0.513	−0.626	−0.596	−0.620	
		ΔQ	+0.225	+0.410	+0.297	+0.327	+0.303	
		Spin	+0.267	+0.473	+0.355	+0.385	+0.364	
	H2	Q	−0.247	−0.434	−0.322	−0.360	−0.343	
		ΔQ	+0.676	+0.489	+0.601	+0.563	+0.580	
		Spin	+0.732	+0.529	+0.643	+0.607	+0.623	

fluorine atoms near the surface have a trend to move inward. The charge difference between the surface and bulk H1 atoms reaches to $0.108e$ is more pronounced than that of other surface atoms, implicating the stronger surface effect on the *H* center than that on other surface fluorine atoms. Further analysis of effective charges demonstrates that this electron transfer is mainly due to the p_z electrons in outer orbital shells. For the *H* center in the deeper layers, i.e., cases 2, 3, and 4, the charge distributions between two fluorine atoms are similar to that of the bulk *H* center. Unlike the case 1, for the case 0, the electron distribution between H1 and H2 in the *H* center is even more unbalanced than that of the bulk *H*-center system, whereas the total charge of the *H* center $(-0.945e)$[28] is very close to the value of case 1 $(-0.947e)$, being also smaller than the bulk *H*-center charge. It is obvious that the top atom of the *H* center for the case 0 is H2 instead of H1, which is different from the case 1, leading to the electrons belonging to H2 having a more remarkable inward transfer. So, this electron distribution polarization of the *H* center for the case 0 also can be explained by the fact that some electrons belonging to surface atoms move inward due to the surface effect.

The localization of the unpaired electron at the *H* center is clearly shown in the spin density map of BaF_2 (see Fig. 4). From the spin density map we can see that, for the case 1, the spin polarization of the neighbor atoms almost disappear and the spin densities of H1 and H2 are closed. Statistically, the unpaired electron approximately lies on both F atoms of the *H* center equally. However, the spin density map for the case 0 is quite different from the case 1 and shows a more distinct spin polarization on H2. Additionally, the spin density of the *H* center looks like a spindle-shaped pattern, which suggests the unpaired electron mainly consisting of *p* orbitals. Further analysis about the direction of spindle axis (*Z* direction) indicates that the projected p_z orbitals form the hole. As mentioned before, the total charge of the *H* center in surface case is smaller than the bulk *H*-center charge. However, the total surface *H*-center spin $(+0.999e$ and $+1.002e$ for the cases 0 and 1, respectively) is by around 1.0% and 1.3% larger than the bulk *H*-center spin $(+0.989e)$,[28] implicating a stronger spin polarization of the surface *H* center. Table II also lists the *H*-center spins of other cases. We can see that their spins are close to the spin of bulk *H* center (H1: $+0.363e$, H2: $+0.626e$)[28] and there is no remarkable surface effect on other cases.

C. Band structure of surface *H* centers

Next, we calculated the band structures of surface *H* centers in BaF_2. BaF_2 with *H* centers exhibits optical absorption, centered around 3.76 eV.[26] Our calculated results for defect levels (see Fig. 5) allow us to explain this experimentally observed optical absorption qualitatively. In the one-electron approximation scheme, the experimentally observed optical

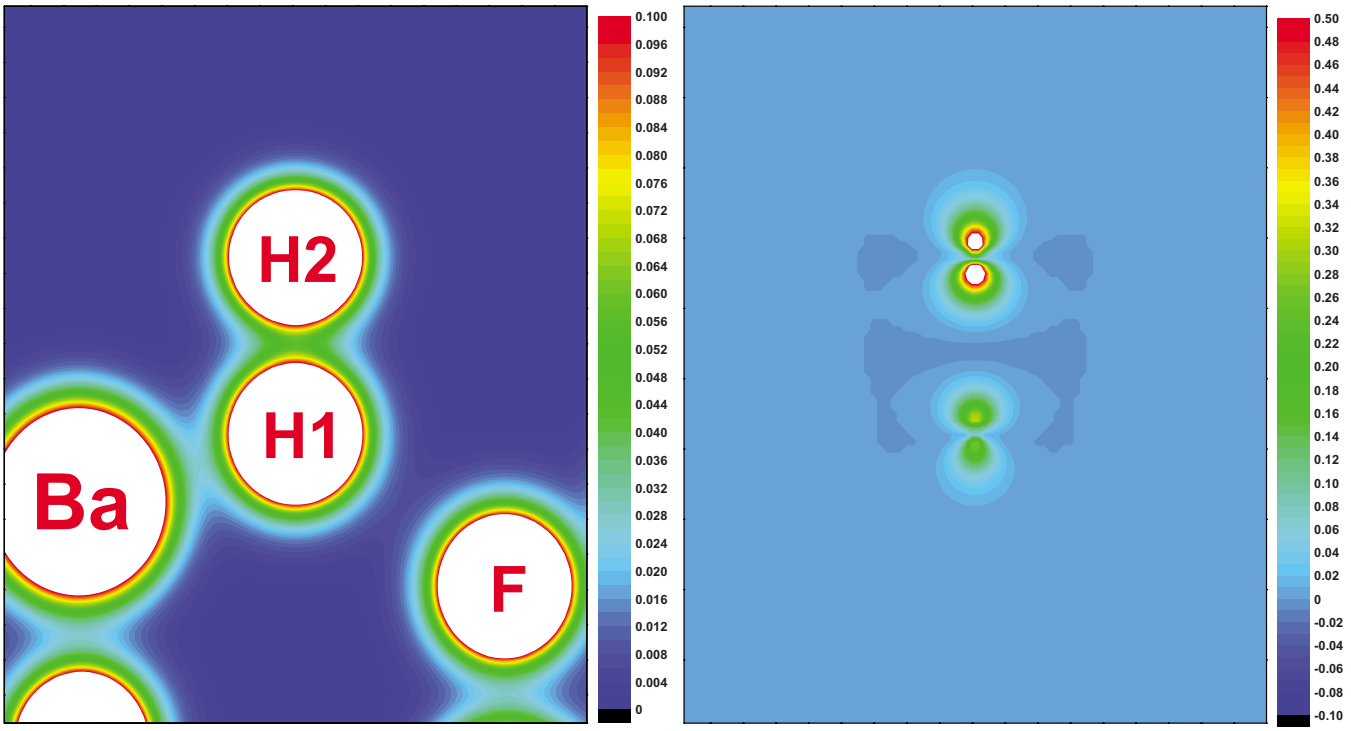

(a)

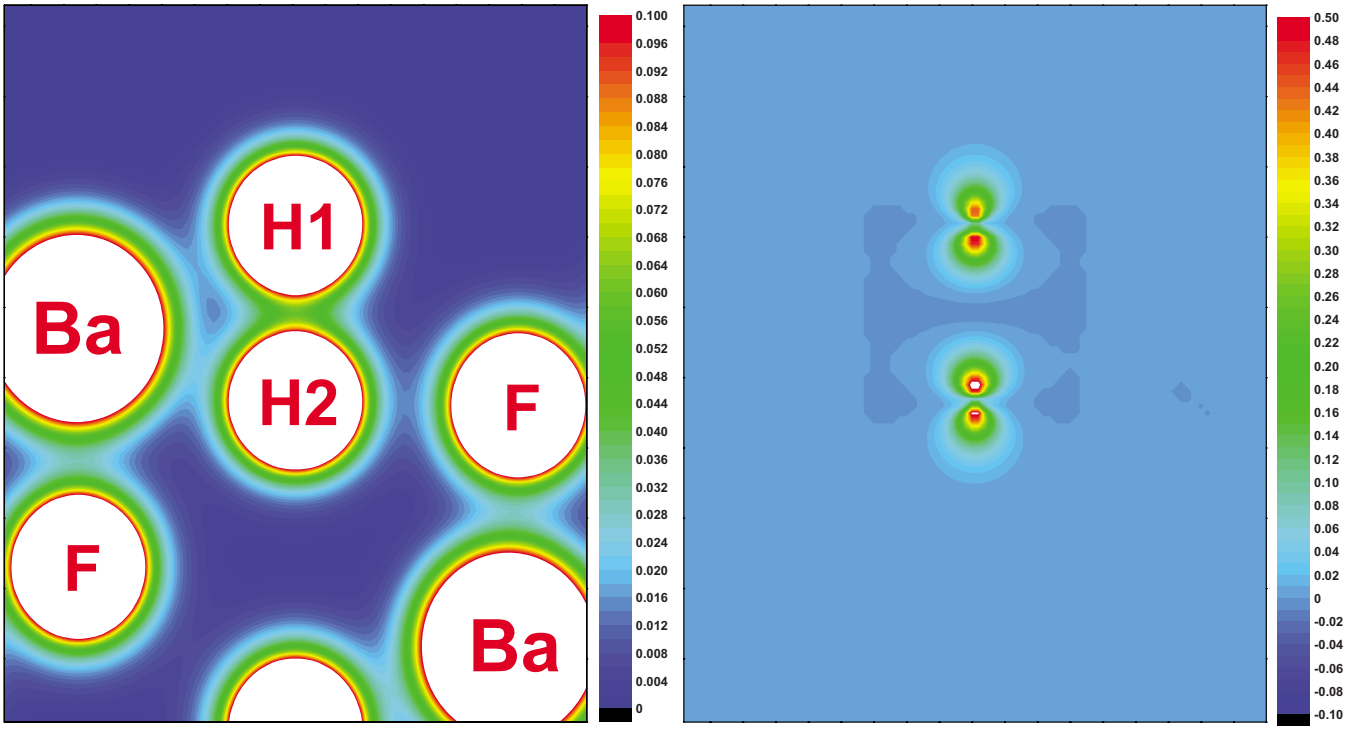

(b)

FIG. 4. (Color online) Electron density (left) and spin density (right) contours in the YZ plane of BaF_2 with a surface H center from side view, being from 0 e/bohr^3 to 0.1 e/bohr^3 with a linear contour spacing of 0.004 e/bohr^3 and from −0.1 e/bohr^3 to +0.5 e/bohr^3 with a linear spacing of 0.02 e/bohr^3, respectively. The upper two maps and lower two maps indicate the case 0 and case 1, respectively.

absorption could be due to an electron transfer from the H-center ground state, to the empty band at β spin induced by a hole localized on the H center (see Fig. 5). The corresponding calculated value is 2.95 eV for the BaF_2 bulk H-center system according to our previous work,[28] which is reasonable, however, is underestimated with respect to the experimental result. As already explained in our previous work,[35] that the recent schemes based on the Bethe-Salpeter

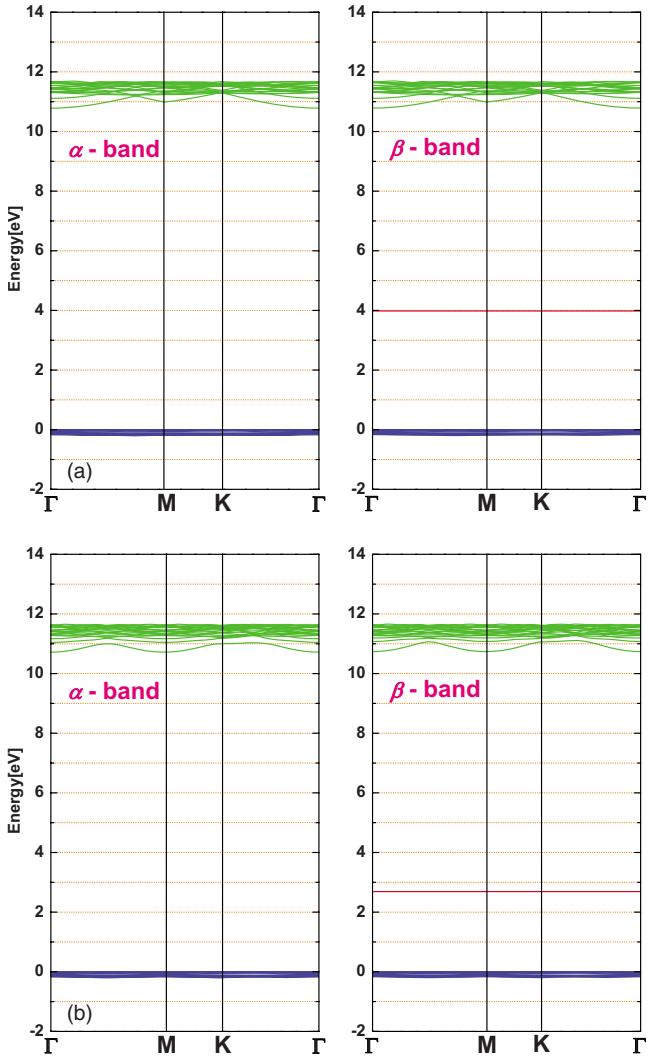

FIG. 5. (Color online) Calculated B3PW band structures for the 108-atom supercell modeling the surface *H* center in BaF_2. The upper and lower panels denote the case 0 and case 1, respectively. α and β denote the up- and down-spin bands, respectively. Fermi energy is shifted to zero eV.

equation in many body perturbation theory give a much better description of certain excited state properties. For an *H*-center system, as mentioned before, there is an unpaired electron localized on the *H* center. The presence of the unpaired electron is also revealed by the band structure of the defective system given in Fig. 5. Unlike the *F*-center case,[20,21] the bound unpaired electron level labeled α band lies in the gap, but very closes to the top of valence bands

TABLE III. Direct optical band gaps (eV) ($\Gamma \rightarrow \Gamma$) for surface *H*-center systems in the cases 0 and 1.

	Case 0		Case 1	
Gaps	α	β	α	β
VB→H		3.99		2.70
VB→CB	10.79	10.79	10.73	10.74

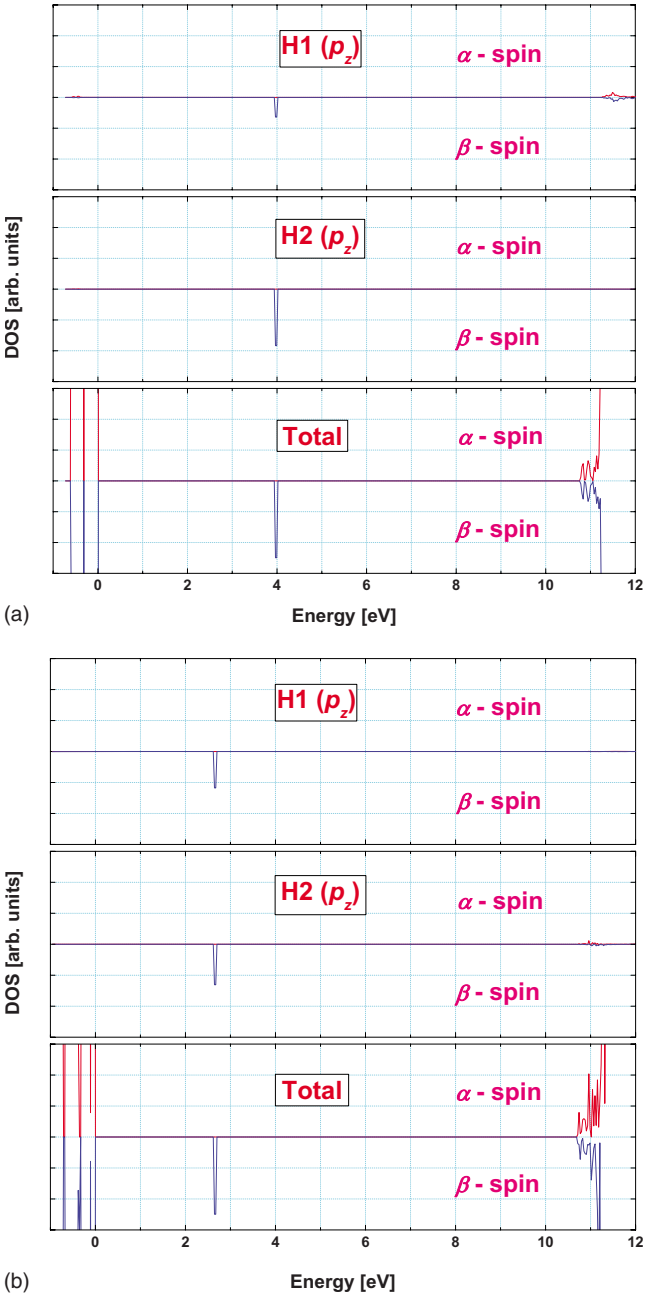

FIG. 6. (Color online) Total and projected density of states (DOS) for surface *H* centers in the (111) BaF_2 surface. The upper and lower pictures indicate the case 0 and case 1, respectively. α and β denote the up- and down-spin states, respectively. Fermi energy is shifted to zero eV.

(VB), as we can see in the α-spin band structure in Fig. 5. The empty level induced by a hole localized on the *H* center appears in the β-spin band structure above the VB top. Because of the selection rules, the electron transition from the α occupied band to the β unoccupied band is forbidden. Therefore, the optical absorption mentioned before could be due to an electron transfer from the β-VB top to the β-empty level, induced by a hole localized on the *H* center.

The optical band gaps of the surface *H*-center systems are shown in Table III. For both cases, all the band gaps between VB and conduction bands (CB) at Γ point are smaller than

those of the bulk *H*-center system (11.11 eV for α and β band structures),[28] which is similar to the phenomenon that the surface effect narrows the band gap of perfect BaF_2 crystal. For the case 1, the β defect level induced by the hole on the *H* center lies 2.70 eV above the CB top, being smaller than the corresponding value in the bulk *H*-center system by 0.25 eV. We also calculated the band gaps of other deeper *H*-center cases and their values are comparable to the gap of case 1. On the other hand, the defect level for the case 0 is quite different from the case 1 and located 3.99 eV above the VB top, magnified greatly by 1.04 eV (around 35%) and 1.29 eV (around 48%) with respect to the gaps of bulk *H*-center system and case 1, respectively. Whereas the VB-CB gap of case 0 does not change nearly, suggesting a marked hole-level movement toward CB. It has been known that the hole is on the interstitial fluorine and for the case 0, this fluorine atom is outside the surface, so the surface effect on this hole is more pronounced than on the hole inside the surface, namely, the case 1, being near the lower sublayer of the first layer.

To further investigate the electronic structure and electron transition in a surface *H*-center system, we calculated density of states (DOS) of surface *H*-center systems. The total and projected DOS of surface *H* centers in BaF_2 are displayed in Fig. 6. Our former work regarding bulk *H* centers[28] showed that H1 and H2 *p* orbitals form the β-hole band, and the H2 does the major contribution. Because of the isotropic symmetry of projected *p* orbitals in BaF_2 bulk, p_x, p_y, and p_z orbitals of the *H* center are equivalent in contribution to the formation of β-hole band. Nevertheless, this symmetry is broken by the (111)-terminated surface and p_z orbitals are not equivalent with p_x and p_y orbitals. So, according to our DOS calculations, we found that for surface *H*-center systems, the β-hole band mainly consists of p_z orbitals of the *H* center, as we can see Fig. 6. As spin density discussed before, the spin pattern in the map looks like a spindle with a *Z*-axis direction (vertical to the surface), which is a typical *p*-shape electron cloud, and our DOS calculations are in accordance with the previous spin density discussion obviously. From Fig. 6, the H1 peak is much smaller than the H2 peak for the case 0, whereas for the case 1 they are similar, also being in agreement with former view that the hole mainly locates on H2 for the case 0 and almost equally on H1 and H2 for the case 1.

In comparison with other defects investigated,[20–24,35] the defect level induced by *H* centers in the α band structure is extremely close to the VB top. We suggest that it is due to this occupied α defect level also consisting mainly of F *p* orbitals, which form the VB top in both perfect and defective crystals. However, other kinds of defect bands, unlike the *H*-center case, are induced by other impurity species, such as *F* centers (an electron trapped in an anion vacancy), hydrogen atoms, and oxygen atoms.

IV. CONCLUSIONS

We applied the first-principles approach within the DFT-B3PW hybrid scheme to calculations on surface *H* centers in BaF_2. Several surface *H*-center configurations were studied and we found that the cases 0 and 1 are the energetically most favorable configurations for surface *H*-center systems, suggesting a trend of *H* centers locating near the surface. The surface effect on *H*-center length is not pronounced, whereas on the relaxation of surface atoms is remarkable. According to our calculations, for the case 0, the hole is mainly localized on the interstitial fluorine, in agreement with the result of bulk *H*-center case, whereas for the case 1, the effective charges of H1 and H2 are so closed that we could not indicate definitely on which fluorine atom the hole is localized. Spin density study shows that an unpaired electron with a spindle-shaped electron cloud, implicating a p_z unpaired electron, localized around the *H* center.

The band structures of surface *H* centers indicate that there is a defect level induced by *H* centers in the gap between VB and CB in the β-spin band structure, however, in the α-spin band structure, the defect level is very close to the top of VB. According to our calculations, the β-hole bands lie 3.99 and 2.70 eV above the top of VB for the cases 0 and 1, respectively. This gap of the case 0 is much larger than the corresponding value in the bulk *H*-center case.

The analysis of DOS calculations clearly reveals that the β-hole band is primarily composed of p_z orbitals localized on the *H* center, as a result of the broken symmetry of *p* orbitals, also being in agreement with previous spin discussion. DOS investigations dealing with other atoms suggest that the vanish of defect levels in the α band gap between VB and CB is due to this occupied α defect level also consisting mainly of F *p* orbitals, which form the VB top in both perfect and defective crystals. However, other kinds of defect bands, unlike the *H*-center case, are induced by other impurity species, such as *F* centers, hydrogen atoms, and oxygen atoms.

*rajia@uni-wuppertal.de

[1] K. Kawano, T. Ohya, T. Tsurumi, K. Katoh, and R. Nakata, Phys. Rev. B **60**, 11984 (1999).
[2] N. Sata, K. Eberman, K. Eberl, and J. Maier, Nature (London) **408**, 946 (2000).
[3] J. Barth, R. L. Johnson, M. Cardona, D. Fuchs, and A. M. Bradshaw, Phys. Rev. B **41**, 3291 (1990).
[4] R. Bennewitz, D. Smith, and M. Reichling, Phys. Rev. B **59**, 8237 (1999).
[5] M. Catti, R. Dovesi, A. Pavese, and V. R. Saunders, J. Phys.: Condens. Matter **3**, 4151 (1991).
[6] W. Y. Ching, F. Q. Gan, and M. Z. Huang, Phys. Rev. B **52**, 1596 (1995).
[7] N. H. de Leeuw and T. G. Cooper, J. Mater. Chem. **13**, 93 (2003).
[8] N. H. de Leeuw, J. A. Purton, S. C. Parker, G. W. Watson, and G. Kresse, Surf. Sci. **452**, 9 (2000).
[9] A. S. Foster, C. Barth, A. L. Shluger, R. M. Nieminen, and M.

Reichling, Phys. Rev. B **66**, 235417 (2002).
[10] F. Q. Gan, Y. N. Xu, M. Z. Huang, W. Y. Ching, and J. G. Harrison, Phys. Rev. B **45**, 8248 (1992).
[11] A. Jockisch, U. Schroder, F. W. Dewette, and W. Kress, J. Phys.: Condens. Matter **5**, 5401 (1993).
[12] M. Letz and L. Parthier, Phys. Rev. B **74**, 064116 (2006).
[13] M. Merawa, M. Llunell, R. Orlando, M. Gelize-Duvignau, and R. Dovesi, Chem. Phys. Lett. **368**, 7 (2003).
[14] V. E. Puchin, A. V. Puchina, M. Huisinga, and M. Reichling, J. Phys.: Condens. Matter **13**, 2081 (2001).
[15] A. V. Puchina, V. E. Puchin, E. A. Kotomin, and M. Reichling, Solid State Commun. **106**, 285 (1998).
[16] G. W. Rubloff, Phys. Rev. B **5**, 662 (1972).
[17] K. Schmalzl, D. Strauch, and H. Schober, Phys. Rev. B **68**, 144301 (2003).
[18] M. Verstraete and X. Gonze, Phys. Rev. B **68**, 195123 (2003).
[19] X. Wu, S. Qin, and Z. Y. Wu, Phys. Rev. B **73**, 134103 (2006).
[20] H. Shi, R. I. Eglitis, and G. Borstel, Phys. Rev. B **72**, 045109 (2005).
[21] H. Shi, R. I. Eglitis, and G. Borstel, J. Phys.: Condens. Matter **18**, 8367 (2006).
[22] H. Shi, R. I. Eglitis, and G. Borstel, J. Phys.: Condens. Matter **19**, 056007 (2007).
[23] H. Shi, R. I. Eglitis, and G. Borstel, Comput. Mater. Sci. **39**, 430 (2007).
[24] R. Jia, H. Shi, and G. Borstel, Phys. Rev. B **78**, 224101 (2008).
[25] T. P. P. Hall, A. Leggeat, and J. W. Twidell, J. Phys. C **2**, 1590 (1969).
[26] J. H. Beaumont, W. Hayes, D. L. Kirk, and G. P. Summers, Proc. R. Soc. London, Ser. A **315**, 69 (1970).
[27] W. Hayes, *Crystals with The Fluorite Structure: Electronic, Vibrational, and Defect Properties* (Clarendon Press, Oxford, 1974).
[28] R. Jia, H. Shi, and G. Borstel, J. Phys.: Condens. Matter **22**, 055501 (2010).
[29] R. Dovesi, V. R. Saunders, C. Roetti, R. Orlando, C. M. Zicovich-Wilson, F. Pascale, B. Civalleri, K. Doll, N. M. Harrison, I. J. Bush, Ph. D'Arco, and M. Llunell, *CRYSTAL06 User's Manual* (University of Torino, Italy, 2008).
[30] S. Piskunov, E. Heifets, R. I. Eglitis, and G. Borstel, Comput. Mater. Sci. **29**, 165 (2004).
[31] R. I. Eglitis, S. Piskunov, E. Heifets, E. A. Kotomin, and G. Borstel, Ceram. Int. **30**, 1989 (2004).
[32] P. J. Hay and W. R. Wadt, J. Chem. Phys. **82**, 299 (1985).
[33] H. J. Monkhorst and J. D. Pack, Phys. Rev. B **13**, 5188 (1976).
[34] C. Pisani, *Quantum-Mechanical Ab initio Calculations of the Properties of Crystalline Materials*, Lecture Notes in Chemistry Vol. 67 (Springer, Berlin, 1996).
[35] R. Jia, H. Shi, and G. Borstel, Comput. Mater. Sci. **43**, 980 (2008).